Covering dynamical systems: Twofold covers

Christophe Letellier

CORIA UMR 6614—Université de Rouen, Place Emile Blondel, F-76821 Mont Saint-Aignan Cedex, France

Robert Gilmore[†]

Laboratoire de Physique des Lasers Atomes et Molécules UMR CNRS 8523, Centre d'Études et de Recherches Lasers et Applications, Université des Sciences et Technologies de Lille, F-59655 Villeneuve d'Ascq Cedex, France

We study the relation between a dynamical system, which is unchanged (equivariant) under a discrete symmetry group $\mathcal{G}$ and another locally identical dynamical system with no residual symmetry. We also study the converse mapping: lifting a dynamical system without symmetry to a multiple cover, which is equivariant under $\mathcal{G}$. This is done in $\mathbb{R}^3$ for the two element rotation and inversion groups. Comparisons are done for the equations of motion, the strange attractors that they generate, and the branched manifolds that classify these strange attractors. A dynamical system can have many inequivalent multiple covers, all equivariant under the same symmetry group $\mathcal{G}$. These are distinguished by the value of a certain topological index. Many examples are presented. A new global bifurcation, the "peeling bifurcation," is described.

I. INTRODUCTION

Many dynamical systems are properly described by amplitudes (optics, classical electrodynamics, quantum mechanics, quantum optics, laser physics), but only intensities are measured. It is then possible to infer chaotic dynamics from the behavior of the intensities. However, at the level of amplitudes, the chaotic dynamics that takes place is more complicated. Some information is "squared away" in the transition from an amplitude description to a description in terms of intensities. More properly speaking, intensity dynamics is an "image" of amplitude dynamics; amplitude dynamics is a "multiple cover" of intensity dynamics. The present paper is designed to respond to the question: "What spectrum of dynamical behavior of the amplitudes is compatible with the observed chaotic behavior of the intensities?"

This is an important particular case of the "cover and image" dynamical system problem. It has long been known that there is a 2→1 relation between the Lorenz [1] and Rössler [2] dynamical systems [3]. In fact, Rössler introduced his equations in order to simplify the study of chaotic dynamics. He viewed his equations as "the square root" of the Lorenz equations, in analogy with Dirac's view of his equations as "the square root" of the Schrödinger equation. In this sense, the Lorenz system is a double cover of the Rössler system. Conversely, there is a 2→1 mapping of a Lorenz strange attractor down to a Rössler-like strange attractor. This 2→1 projection is most easily visualized by viewing the Lorenz attractor along the $x=y$ axis. From this perspective, the two foci and their associated lobes fall on top of each other. There appear to be only two fixed points, and the attractor takes on the qualitative appearance of a Rössler attractor.

In this paper, we discuss the relation between cover and image dynamical systems. We do this only for dynamical systems in $\mathbb{R}^3$, and only for covering dynamical systems unchanged by (equivariant under) a discrete symmetry group $\mathcal{G}$ of order two. The general setup for the cover-image projection is presented in Sec. II. In Sec. III we describe projections of $\mathcal{R}_z(\pi)$ equivariant systems to their image equations. This is done explicitly for the Lorenz and the Burke and Shaw systems. These procedures are applied to $\mathcal{P}$ (inversion) invariant systems in Sec. IV, specifically to the induced Lorenz and to the Kremliovsky systems. Comparisons are made between the equations, the strange attractors which they generate, and the templates, or branched manifolds, which identify these strange attractors [4].

The inverse problem ("lift problem") of creating a covering dynamical system with symmetry group $\mathcal{G}$ from an image dynamical system without symmetry is discussed in Secs. V and VI. In Sec. V we construct the equations for one of the rotation equivariant double covers of the Rössler system. An image can have many inequivalent covers, all with the same symmetry group $\mathcal{G}$. These inequivalent covers are distinguished among themselves by the values of a topological index **n**. Four inequivalent two fold covers with symmetry group $\mathcal{R}_z(\pi)$ are created for the Smale horseshoe template in the remainder of Sec. V, three covers with symmetry group $\mathcal{P}$ are constructed in Sec. VI. In Sec. VII, a new global bifurcation is described.

In Sec. VIII we describe how to construct a branched manifold that describes the twofold cover of a strange attractor starting from the branched manifold of the image attractor, the symmetry group $\mathcal{G}$, and the topological index **n**. This is done both from the diagram and the algebraic description of the templates. Section IX contains a brief summary and discussion of these results.

II. PROCEDURE

The system of dynamical equations

$$\dot{x}=F_1(x,y,z) \tag{1a}$$

[†]Permanent address: Physics Department, Drexel University, Philadelphia, PA 19104.

$$\dot{y} = F_2(x,y,z), \tag{1b}$$

$$\dot{z} = F_3(x,y,z), \tag{1c}$$

which is invariant under the group $\mathcal{G}$ of order 2, is mapped into a locally equivalent dynamical system

$$\dot{u} = g_1(u,v,w), \tag{2a}$$

$$\dot{v} = g_2(u,v,w), \tag{2b}$$

$$\dot{w} = g_3(u,v,w) \tag{2c}$$

without any residual symmetry. This is done by constructing a nonlinear coordinate transformation

$$u = u(x,y,z), \tag{3a}$$

$$v = v(x,y,z), \tag{3b}$$

$$w = w(x,y,z) \tag{3c}$$

in which the coordinates (u,v,w) are invariant under $\mathcal{G}$. The coordinates (u,v,w) are linear combinations of elementary polynomials in (x,y,z) of degree $\leq |\mathcal{G}|$ [5], which are invariant under $\mathcal{G}$. The invariant dynamical system equations $\dot{u}_i = g_i(\mathbf{u})$ are determined in a straightforward way from

$$\frac{du_i}{dt} = \frac{\partial u_i}{\partial x_j}\frac{dx_j}{dt} = \frac{\partial u_i}{\partial x_j}F_j(\mathbf{x}) = g_i(\mathbf{u}). \tag{4}$$

These equations are called the projected or image equations.

It is possible to construct $|\mathcal{G}|$ fold covers of an invariant dynamical system with symmetry group $\mathcal{G}$ from an invariant system (in u_i) by inverting the Jacobian

$$\frac{dx_i}{dt} = \frac{\partial x_i}{\partial u_j}\frac{du_j}{dt} = \left(\frac{\partial u}{\partial x}\right)^{-1}_{ij} g_j(\mathbf{u}) = F_i(\mathbf{x}). \tag{5}$$

These equations are called the lifted or covering equations. The Jacobian $(\partial u/\partial x)$ has zeroes along some curves or surfaces in $\mathbb{R}^3$. It is therefore necessary to treat the singularities of $(\partial x/\partial u)$ carefully. As a result of these singularities, an invariant dynamical system $\dot{u}_i = g_i(\mathbf{u})$ can have many different covering dynamical systems, which are equivariant under the same group $\mathcal{G}$. These inequivalent covers are distinguished by a topological index.

Three inequivalent two element groups $\mathcal{G}$ exist in $\mathbb{R}^3$. These are the groups of

Reflections $\quad \sigma_z : (x,y,z) \rightarrow (x,y,-z),$

Rotations $\mathcal{R}_z(\pi):(x,y,z)\rightarrow(-x,-y,z),$

Inversions $\quad \mathcal{P}:(x,y,z)\rightarrow(-x,-y,-z).$

In this paper we study only the latter two. The reason is that strange attractors with reflection symmetry must be disconnected. We are interested in the nontrivial case where the equivariant attractors are connected.

We study the projection—lift problem at three levels: the equations themselves, the strange attractors generated by these equations, and the branched manifolds that characterize the attractors.

III. PROJECTIONS OF ROTATION EQUIVARIANT SYSTEMS

The elementary polynomials in (x,y,z) of degree up to two $(=|\mathcal{G}|)$ invariant under $\mathcal{R}_z(\pi)$ are z, x^2, xy, and y^2 [5]. The following coordinate transformation is convenient

$$u = x^2 - y^2, \tag{6a}$$

$$v = 2xy, \tag{6b}$$

$$w = z. \tag{6c}$$

This transformation "mods out" the rotation symmetry. We now apply this projection transformation to two dynamical systems with rotational symmetry.

A. Lorenz equations

The Lorenz equations [1]

$$\dot{x} = -\sigma x + \sigma y, \tag{7a}$$

$$\dot{y} = Rx - y - xz, \tag{7b}$$

$$\dot{z} = -bz + xy \tag{7c}$$

are equivariant under $\mathcal{R}_z(\pi)$. An invariant image of the Lorenz system can be constructed using the image equations (4) and the transformation (6). This results in the "proto-Lorenz equations" [6].

$$\dot{u} = (-\sigma-1)u + (\sigma-R)v + vw + (1-\sigma)\rho, \tag{8a}$$

$$\dot{v} = (R-\sigma)u - (\sigma+1)v - uw + (R+\sigma)\rho - \rho w, \tag{8b}$$

$$\dot{w} = -bw + \tfrac{1}{2}v, \tag{8c}$$

where $\rho = \sqrt{u^2+v^2}$.

The flows generated by the Lorenz and proto-Lorenz equations are shown in Fig. 1. The branched manifolds, which describe these flows, are also shown in this figure.

The branched manifold shown for the Lorenz flow can be deformed to the more familiar branched manifold representation by giving the right-hand lobe a half-twist, with the top coming out of the page [4]. The branched manifold shown for the proto-Lorenz flow is equivalent to the branched manifold for a Smale horseshoe.

B. Burke and Shaw equations

The Burke and Shaw equations [7]

$$\dot{x} = -S(x+y), \tag{9a}$$

$$\dot{y} = -y - Sxz, \tag{9b}$$

Equivariant $\mathcal{R}_z(\pi)$ Invariant

Lorenz   Image

Equivariant $\mathcal{R}_z(\pi)$ Invariant
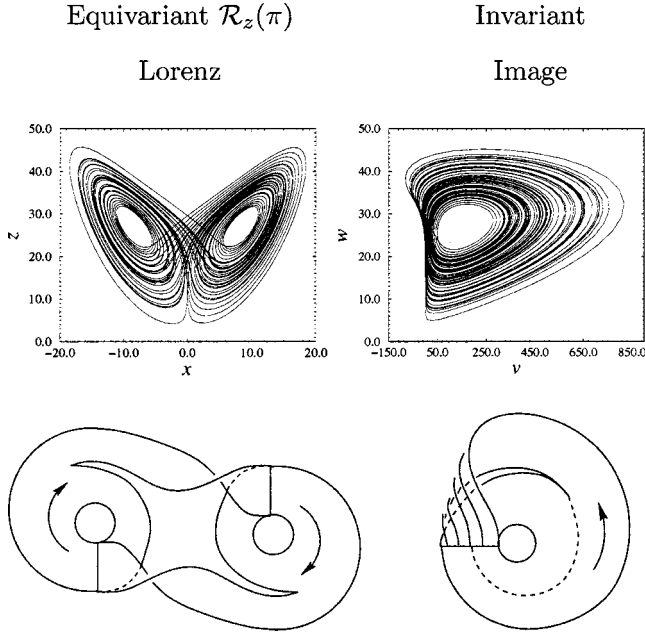
Burke and Shaw   Image

FIG. 1. Top: Strange attractors generated by $\mathcal{R}_z(\pi)$ equivariant Lorenz equations (7) and invariant image equations (8). Parameter values: $\sigma = 10.0$, $R = 28.0$, and $b = 8/3$. Bottom: Branched manifolds for these two strange attractors.

$$\dot{z} = Sxy + \mathcal{V} \qquad (9c)$$

are also equivariant under $\mathcal{R}_z(\pi)$. Under the transformation (6) the image equations are

$$\dot{u} = -(S+1)u - S(1-w)v + (1-S)\rho, \qquad (10a)$$

$$\dot{v} = S(1-w)u - S(1+w)\rho - (S+1)v, \qquad (10b)$$

$$\dot{w} = \frac{S}{2}v + \mathcal{V}, \qquad (10c)$$

where $\rho = \sqrt{u^2 + v^2}$.. The flows generated by the Burke and Shaw dynamical system (9) and its image (10) are shown in Fig. 2. The branched manifolds, which describe these strange attractors, are also shown.

The branched manifold for the projected system is that of a Smale horseshoe with an additional half-twist in the return flow. This is equivalent to a reverse horseshoe.

IV. PROJECTIONS OF INVERSION EQUIVARIANT SYSTEMS

The elementary polynomials in (x,y,z) of degree up to two, which are invariant under $\mathcal{P}$, are xy, yz, zx, x^2, y^2, and z^2. The following coordinate transformation is convenient:

$$u = x^2 - y^2, \qquad (11a)$$

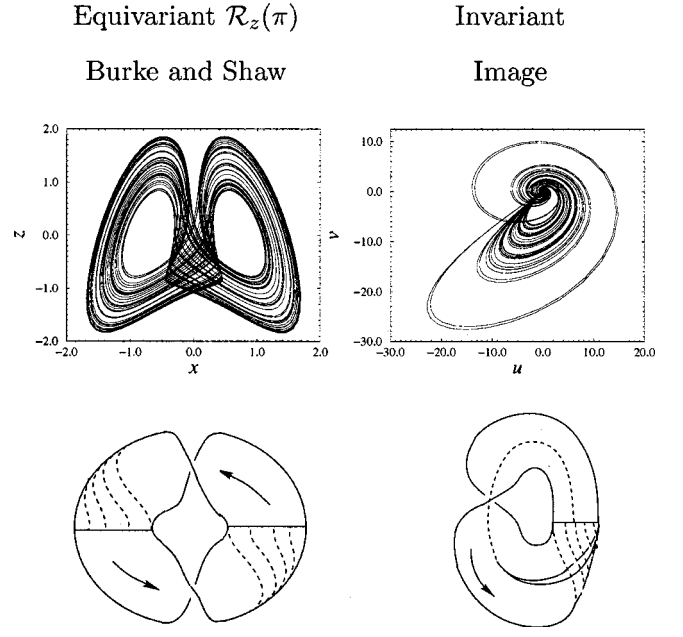$$v = 2xy, \qquad (11b)$$

$$w = (x-y)z. \qquad (11c)$$

FIG. 2. Top: Strange attractors generated by $\mathcal{R}_z(\pi)$ equivariant Burke and Shaw equations (9) and invariant image equations (10). Parameter values: $V = 4.271$, and $S = 10.0$. Bottom: Branched manifolds for these two strange attractors.

This transformation ''mods out'' the inversion symmetry. We apply this projection to two dynamical systems with inversion symmetry.

A. Induced Lorenz system

The induced Lorenz system [3] occurs naturally in all attempts to analyze scalar data, $s(t)$, behaving like the x or y variable in the Lorenz system. Specifically, if a differential embedding is used to construct a three-dimensional phase space according to

$$X = s(t), \qquad (12a)$$

$$Y = \dot{s}(t), \qquad (12b)$$

$$Z = \ddot{s}(t) \qquad (12c)$$

then the derivative coordinates obey the equations

$$\dot{X} = Y, \qquad (13a)$$

$$\dot{Y} = Z, \qquad (13b)$$

$$\dot{Z} = b\sigma(R-1)X - b(\sigma+1)Y - (b+\sigma+1)Z$$

$$-X^2Y - \sigma X^3 + \frac{Y[(\sigma+1)Y + Z]}{X}, \qquad (13c)$$

The apparent singularity in Eq. (13) is not a difficulty if $Y[(\sigma+1)Y + Z] \approx \mathcal{O}(X)$ as $X \to 0$. That is, the flow passes through the straight line $Y[(\sigma+1)Y + Z] = 0$ in the $X = 0$ plane. The invariant image equations of the induced Lorenz system are too complicated to present here. The flows gen-

Equivariant $\mathcal{P}$
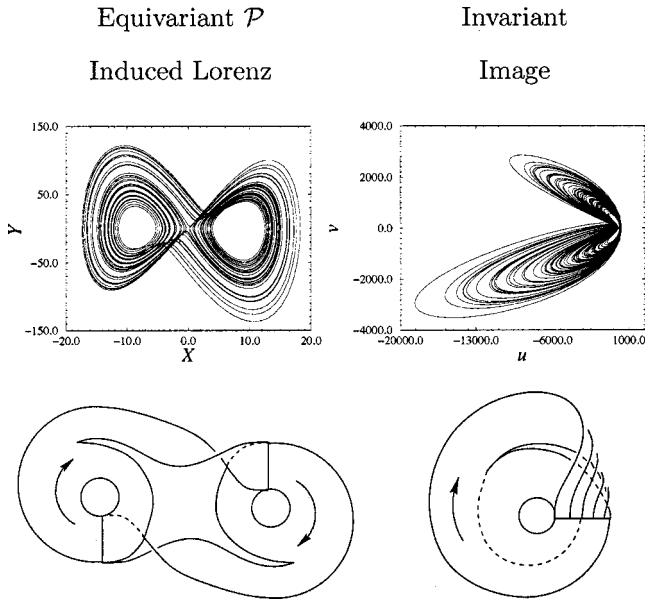
Induced Lorenz

Invariant

Image

FIG. 3. Top: Strange attractors generated by $\mathcal{P}$ equivariant induced Lorenz equations (13) and invariant image equations. Parameter values: $\sigma = 10.0$, $R = 28.0$, and $b = 8/3$. Bottom: Branched manifolds for these two strange attractors.

erated by the induced Lorenz system and the invariant image are shown in Fig. 3. The branched manifolds, which characterize these flows, are shown in the same figure.

B. Kremliovsky equations

Kremliovsky modified the Rössler equations [cf. Eq. (15) below] by modifying the $\dot{z}$ equation [$b \to bx$, $w(u-c) \to z(x^2-c)$] to construct a three-dimensional dynamical system [8]

$$\dot{x} = -y - z, \tag{14a}$$

$$\dot{y} = x + ay, \tag{14b}$$

$$\dot{z} = bx + z(x^2 - c), \tag{14c}$$

which is equivariant under $(x,y,z) \to (-x,-y,-z)$. The invariant image of this dynamical system is also too complicated to present here. The flows generated by the Kremliovsky system (14) and its invariant image are shown in Fig. 4. In this figure we also present the branched manifolds that characterize these strange attractors.

V. LIFTS TO ROTATION INVARIANT SYSTEMS

A double cover for the Rössler system

$$\dot{u} = -v - w, \tag{15a}$$

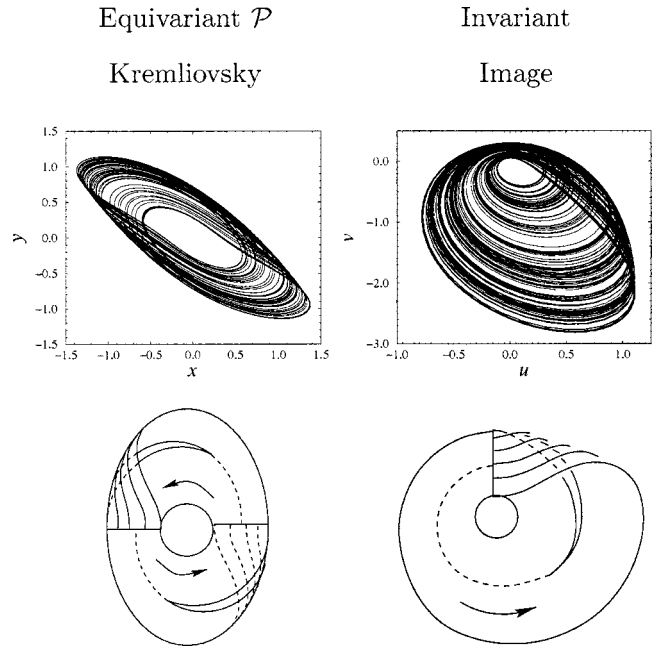$$\dot{v} = u + av, \tag{15b}$$

$$\dot{w} = b + w(u - c) \tag{15c}$$

Equivariant $\mathcal{P}$

Kremliovsky

Invariant

Image

FIG. 4. Top: Strange attractors generated by $\mathcal{P}$ equivariant Kremliovsky equations (14) and invariant image equations. Parameter values: $a = 0.911$; $b = 0.9547623431$; $c = 2.192954632$. Bottom: Branched manifolds for these two strange attractors.

can be constructed using the lift equations (5) and the transformation (6). The resulting dynamical system equations with twofold rotational symmetry are

$$\dot{x} = \frac{1}{2\rho^2} [-\rho^2 y + x(2ay^2 - z)], \tag{16a}$$

$$\dot{y} = \frac{1}{2\rho^2} [\rho^2 x + y(2ax^2 + z)], \tag{16b}$$

$$\dot{z} = b + z(x^2 - y^2 - c), \tag{16c}$$

where $\rho = \sqrt{x^2 + y^2}$. The strange attractors generated by the Rössler equations (15) and the twofold cover (16) are shown in Fig. 5. Also shown in this figure are the branched manifolds for these two strange attractors.

This is not the only double cover of the Rössler system with $\mathcal{R}_z(\pi)$ rotation symmetry. Many other double covers can be constructed, all invariant under $\mathcal{R}_z(\pi)$, all topologically inequivalent to the one shown in Fig. 5 and with each other. We now explain how this can come about.

The transformation (6) mapping $(x,y,z) \to (u,v,w)$ is $2 \to 1$ everywhere except on the z and w axes, where it maps $(0,0,z) \to (0,0,w)$ in a 1-1 way. The Jacobian of the transformation $\partial u_i / \partial x_j$, is singular on the z axis. Within the image space (u,v,w), there is no singularity along the w axis. This allows one to construct several inequivalent covers with the same symmetry group for an invariant dynamical system.

We illustrate this idea for invariant dynamical systems that generate strange attractors classified by a Smale horseshoe template (e.g., the Rössler equations). This template is shown in Fig. 6. Each branch contains one unstable period
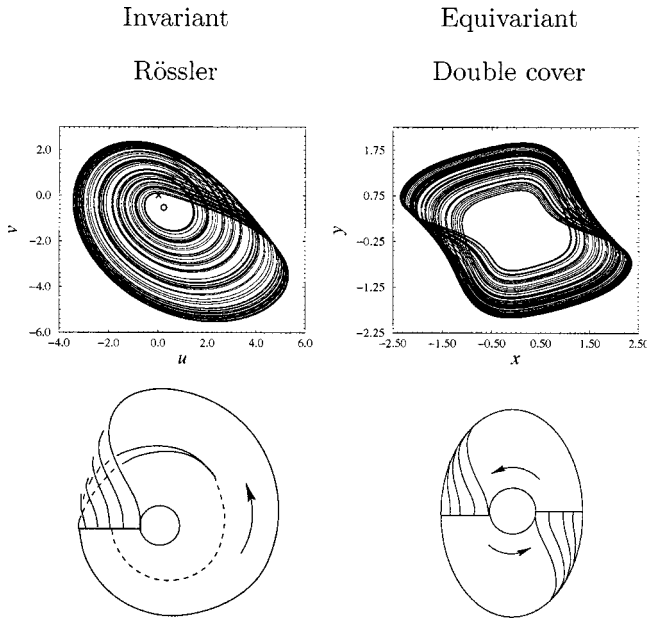
FIG. 5. Top: Strange attractors generated by Rössler equations (15) and twofold cover equivariant under $\mathcal{R}_z(\pi)$ (16). Parameter values: $a=0.415$, $b=2.0$, and $c=4.0$. Bottom: Branched manifolds for these two strange attractors.
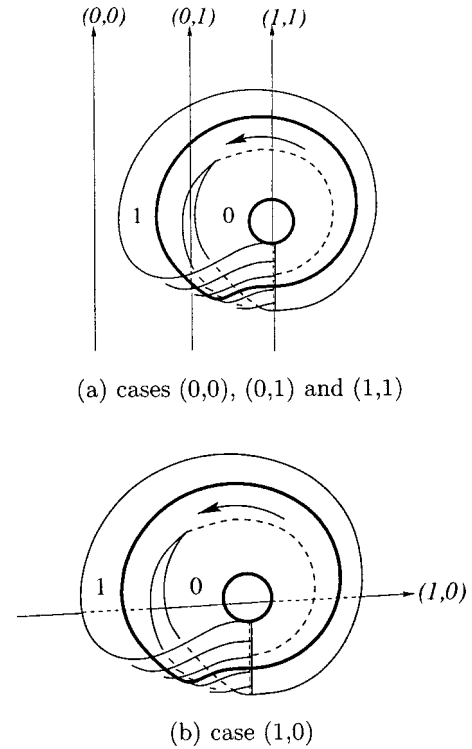

FIG. 6. Two branch Smale horseshoe template. The period one orbit in each branch is shown by a heavy line. Four possible images in (u,v,w) space of the rotation axis $(0, 0, z)$ in (x,y,z) space are shown. They are labeled by their linking numbers (n_0,n_1) with the two period one orbits. These axes have been chosen to be disjoint from the strange attractor's branched manifolds: 0 or 1. (a) The three cases (0,0), (0,1), and (1,1) are shown. (b) In the case (1,0), the rotation axis passes behind branch 1, in front of branch 0, then through the hole in the middle of the attractor and behind both branches.

one orbit. These orbits are shown by heavy lines. The period one orbits and the branches that contain them are indexed by the same labels. In the present case this is the global torsion of the orbit and the branch in which it resides: 0 or 1.

Also shown in Fig. 6 are four possible rotation axes $(u,v,w)=(0,0,w)$. Each of these axes links the two period one orbits in different ways. If we call n_0, n_1 the linking numbers of the period one orbits 0 and 1 with the w axis (closed by a return at ∞), the four cases shown are (0,0), (0,1), (1,0), and (1,1).

The branched manifold, which describes a double cover of the Smale horseshoe template, has four branches. Consider a closed orbit in this covering branched manifold. If its linking number with the z axis is n, then the linking number of the image orbit with the w axis is $2n$. If $n=1$, the orbit in the double cover goes around the z axis once while its image goes around the w axis twice. In particular, if $n_1=1$, then the period one orbit 1 in the Smale horseshoe template cannot be the image of a closed orbit in the cover template. If the orbit in the cover space does not link the z axis, its image orbit does not link the w axis, and vice versa.

In Fig. 7 we show the four double covers of the Smale horseshoe template, which correspond to the four choices of the w axis shown in Fig. 6. Each double cover is equivariant under $R_z(\pi)$.

Each of the branched manifolds in Fig. 7, which covers $\mathcal{SH}$, is invariant under $R_z(\pi)$ and has four branches. These are labeled by an integer (0 or 1), a subscript (l or r), and another symbol (ˆ or ¯). The integer identifies whether the branch in the cover is mapped into branch 0 or 1 in $\mathcal{SH}$. The subscript identifies whether the branch is on the left-or right-hand side of the cover. Under $R_z(\pi)$, $l \to r$ and $r \to l$. The extra symbol has a topological significance. It indicates

whether the image links the rotation axis once (ˆ) or not at all (¯).

We describe in some detail the relation between the branched manifold shown in Fig. 7(b) and its image, the Smale horseshoe template shown in Fig. 6. The cover template has four branches: one ($\bar{0}_l$) entirely in the left lobe, its image ($\bar{0}_r$) under $R_z(\pi)$, one branch ($\hat{1}_l$) extending from the left lobe to the right lobe, and its image ($\hat{1}_r$) under $R_z(\pi)$. Under projection, the image of the two branches $\bar{0}_l,\bar{0}_r$ in the cover template is the branch 0 in the Smale horseshoe template. The branches $\hat{1}_l,\hat{1}_r$ both map to the branch 1 in the horseshoe template. The period one orbit in $\bar{0}_l$ and its counterpart in $\bar{0}_r$ do not link the z axis ($n=0$). Both map to the period one orbit 0 in the horseshoe template, which does not link the w axis ($n_0=0$). There is one period two orbit $\hat{1}_l\hat{1}_r$ in the cover template. This links the z axis once ($n=1$). This period two orbit maps twice onto the period one orbit 1 in the horseshoe template ($\hat{1}_l\hat{1}_r \to 11$), which links the w axis twice ($n=2$). The period one orbit 1 links the w axis once ($n_1=1$).
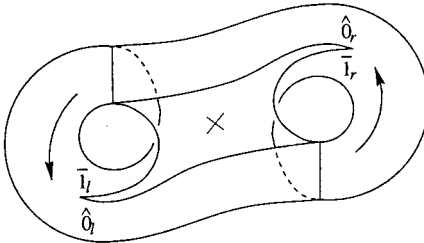
These arguments can be run backwards. Since $n_0=0$, the period one orbit 0 in the horseshoe lifts to two symmetry
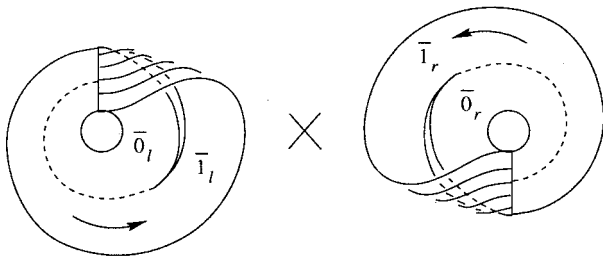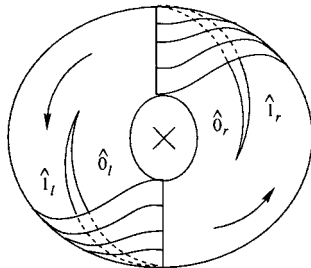
(a) $(n_0, n_1) = (0, 0)$
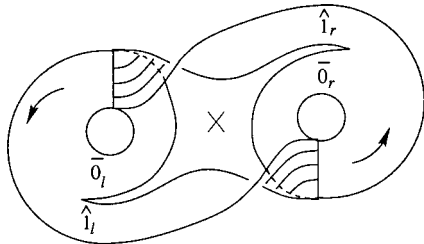
(b) $(n_0, n_1) = (0, 1)$
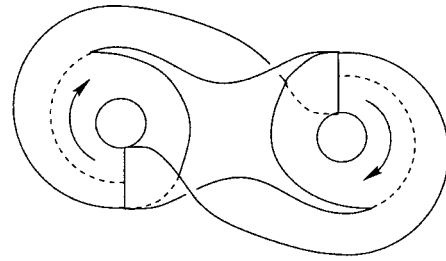

(c) $(n_0, n_1) = (1, 0)$
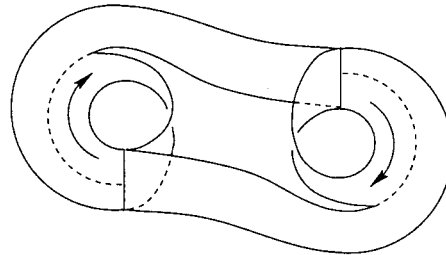

(d) $(n_0, n_1) = (1, 1)$

FIG. 7. Branched manifolds for four inequivalent double covers of the Smale horseshoe template. Each cover is equivariant under rotations by π around an axis through $\times$. The four different double covers are identified by their topological index (n_0, n_1).

(a) $(n_0, n_1) = (0, 1)$

(b) $(n_0, n_1) = (1, 0)$

(c) $(n_0, n_1) = (1, 1)$

FIG. 8. Branched manifolds for three inequivalent connected covers with inversion symmetry of the Smale horseshoe branched template.

shown in Fig. 7 are not topologically equivalent, the dynamical systems they represent are also inequivalent. The lift with $(n_0, n_1) = (0, 0)$ is disjoint and not interesting.

VI. LIFTS TO INVERSION INVARIANT SYSTEMS

The nonlinear transformation (11) has an invariant set, which consists of the union of the z axis and the plane $x - y = 0$. The z-axis component of this invariant set can be treated in exactly the same way as the z axis in the rotational invariant case. The $x - y = 0$ plane does not provide an obstruction to the flow. In Fig. 8 we show three inequivalent double covers of the Smale horseshoe manifold. Each has inversion symmetry and is connected.

VII. A NEW GLOBAL BIFURCATION: PEELING

In Fig. 7(d), the double cover with $(n_0, n_1) = (1, 1)$ exhibits dynamics similar to the strange attractor for the Duffing oscillator [9]. The four branches in this cover $\mathcal{D}$ are $(\hat{0}_l, \hat{1}_l, \hat{1}_r, \hat{0}_r)$. The double cover with $(n_0, n_1) = (0, 1)$ [Fig.

related orbits, $\overline{0}_l$ and $\overline{0}_r$, which do not link the z axis. Since $n_1 = 1$, the period one orbit 1 in the horseshoe lifts to "half a closed orbit" $\hat{1}_l$ or $\hat{1}_r$, which is then closed by adding the complementary symmetry related segment ($\hat{1}_r$ or $\hat{1}_l$). This closed orbit $\hat{1}_l \hat{1}_r$ in the cover links the z axis with $n = 1$. That is, the period "two" orbit 11, with $n = n_1 + n_1 = 2$, lifts to the period two orbit $\hat{1}_l \hat{1}_r$ with $n = 1$.
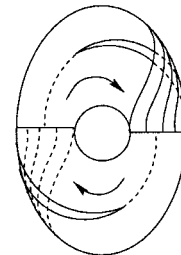
The relation between cover and image branched manifolds for other choices of the topological index (n_0, n_1) are described similarly. Since the four 4-branched manifolds

(a)

(b)
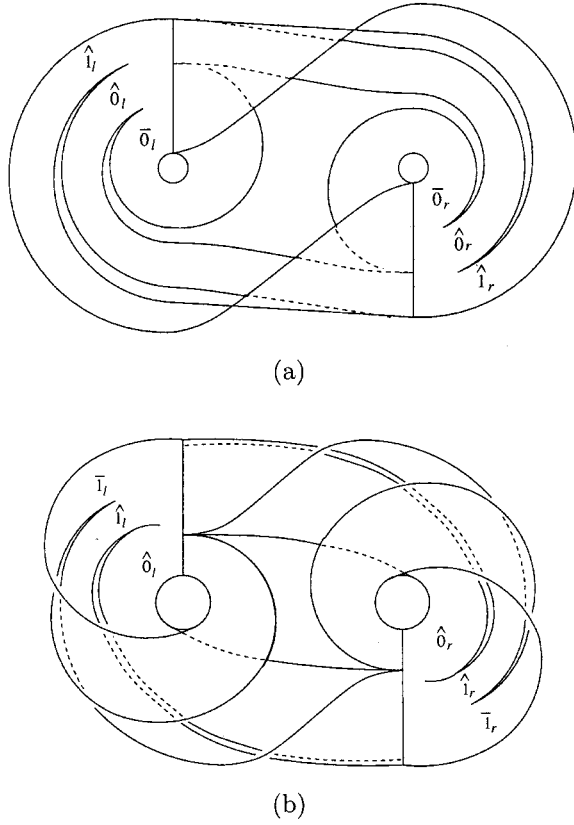
FIG. 9. Double covers of $\mathcal{SH}$ with six branches. The lifts are obtained when the symmetry axis w intersects the branch 0 (a) or 1 (b) of $\mathcal{SH}$.

7(b)] is topologically equivalent to the Lorenz system [1]. The four branches in this cover $\mathcal{L}$ are $(\bar{0}_l, \hat{1}_l, \hat{1}_r, \bar{0}_r)$. Finally, the double cover with $(n_0, n_1) = (0,0)$ consists of two identical copies of the image branched manifold related by rotation symmetry [Fig. 7(a)]. The four branches in this disconnected double cover $2\mathcal{SH}$ are $(\bar{0}_l, \bar{1}_l)$ in the copy on the left and $(\bar{1}_r, \bar{0}_r)$ for the copy on the right.

We now describe the new global bifurcation. Choose the rotation axis w so that $(n_0, n_1) = (1,1)$. Then displace the w axis outward, so that it first intersects the branch 0 of the image Smale horseshoe template $\mathcal{SH}$, then branch 1. The covering templates are shown in Fig. 9. As the rotation axis crosses branch 0 of $\mathcal{SH}$, outer orbit segments in this branch encircle the w axis once, inner segments do not. In the cover, the branches $\hat{0}_{l,r}$ split into two pieces, $\hat{0}_{l,r}$ and $\bar{0}_{l,r}$, depending on where the image occurs under the diffeomorphism (i.e., outside or inside w). The cover branched manifold remains invariant under $R_z(\pi)$ but now has six branches: $(\bar{0}_l, \hat{0}_l, \hat{1}_l, \hat{1}_r, \hat{0}_r, \bar{0}_r)$ [Fig. 9(a)]. This six-branch manifold interpolates between the template $\mathcal{D}$ with four branches and the template $\mathcal{L}$, also with four branches.

A similar perestroika occurs as the rotation axis w crosses branch 1 of $\mathcal{SH}$. The cover branches $\hat{1}_{l,r}$ split into two pieces, $\hat{1}_{l,r}$ and $\bar{1}_{l,r}$, depending on where the image occurs under the diffeomorphism. The covering branched manifold once again has six branches [Fig. 9(b)]. These are now

$(\bar{0}_l, \bar{1}_l, \hat{1}_l, \hat{1}_r, \bar{1}_r, \bar{0}_r)$. This six-branch template interpolates between the template $\mathcal{L}$ with four branches and the disconnected template $2\mathcal{SH}$, with two pairs of branches.

We exhibit this bifurcation explicitly for the Rössler system of equations [2]. Instead of displacing the symmetry axis, we equivalently modify the equations by displacing the origin of coordinates $(u,v,w) \to (u+u_0, v+v_0, w+w_0)$. First, the Rössler is centered through a rigid displacement, i.e., the inner fixed point is moved to the origin of the phase space $\mathbb{R}^3(u,v,w)$. In the translated coordinate system, the equations for this image system are

$$\dot{u} = -v - w - v_0 - w_0, \tag{17a}$$

$$\dot{v} = u + av + u_0 + av_0, \tag{17b}$$

$$\dot{w} = b + w(u + u_0 - c) + w_0 u + w_0(u_0 - c), \tag{17c}$$

where $u_0 = -v_0 = aw_0 = (c - \sqrt{c^2 - 4ab})/2$ are the coordinates of the inner fixed point of the original Rössler system. The system may then be rewritten as

$$\dot{u} = -v - w, \tag{18a}$$

$$\dot{v} = u + av, \tag{18b}$$

$$\dot{w} = \tilde{b}u + w(u - \tilde{c}), \tag{18c}$$

where $\tilde{b} = w_0$ and $\tilde{c} = c - u_0$.

When the origin of coordinates is displaced along the u axis by a quantity equal to μ, the equations for the image system in the translated coordinates are

$$\dot{u} = -v - w, \tag{19a}$$

$$\dot{v} = u + av + \mu, \tag{19b}$$

$$\dot{w} = \tilde{b}(u + \mu) + w(u - \tilde{c} + \mu), \tag{19c}$$

We integrated these equations, and the covering equations obtained from them using Eq. (3), for $(a,b,c) = (0.432, 2.0, 4.0)$ and five values of μ. The covering equations are

$$\dot{x} = \frac{1}{2r^2}[-r^2 y + x(2ay^2 - z) + \mu y], \tag{20a}$$

$$\dot{y} = \frac{1}{2r^2}[r^2 x + y(2ax^2 + z) + \mu x], \tag{20b}$$

$$\dot{z} = \tilde{b}(x^2 - y^2 + \mu) + z(x^2 - y^2 - \tilde{c} + \mu), \tag{20c}$$

where $r = \sqrt{x^2 + y^2}$.

The results are shown in Fig. 10. The strange attractors shown in Fig. 10(a), 10(c), and 10(e) all have four branches and are the double covers of the Rössler attractor with topological indices $(n_0, n_1) = (1,1)$, $(0,1)$, and $(0,0)$. The strange attractor shown in Fig. 10(b) has six branches and interpolates between the attractors $\mathcal{D}$ and $\mathcal{L}$ with $(n_0, n_1) = (1,1)$ and $(0,1)$. The strange attractor shown in Fig. 10(b) also has

(a) $\mu = 0.0$

(b) $\mu = -0.84548$

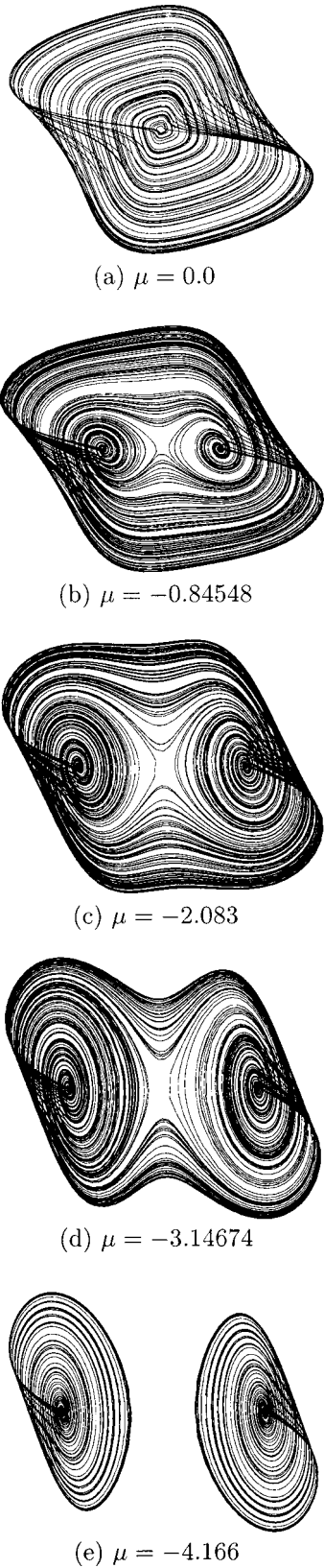(c) $\mu = -2.083$

(d) $\mu = -3.14674$

(e) $\mu = -4.166$

FIG. 10. Five double cover strange attractors for the Rössler equations (48). These are obtained by displacing the origin of coordinates along the u axis.
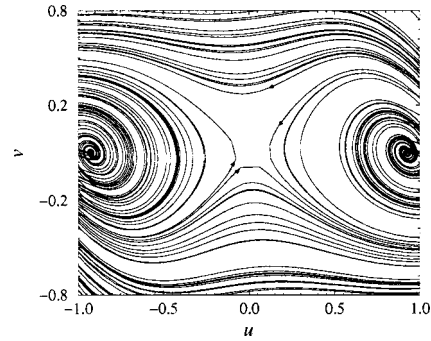

FIG. 11. Deformation of the flow in the double cover when the symmetry axis intersects the strange attractor. The contorted structure is similar to the deformation of an apple skin when the apple is peeled.

six branches and interpolates between the attractors $\mathcal{L}$ and $2\mathcal{SH}$ with $(n_0, n_1) = (0,1)$ and $(0,0)$. The nature of the flow in the neighborhood of the z axis is shown in Fig. 11. The deformation of the flow, which takes place in the covering system, is very similar to the deformation of an apple skin when the apple is peeled. Hence the name for this new global bifurcation (Figure 11).

We emphasize here that the placement of the w axis has no effect on the nature of the flow in the image system. The bifurcation takes place only in the covering dynamical system; the image system remains invariant during the displacement of the symmetry axis.

As the w axis is moved across the branches of the image Smale horseshoe template $\mathcal{SH}$, a systematic reorganization takes place in the lifts of the unstable periodic orbits in $\mathcal{SH}$. When the w axis passes through the center of rotation of $\mathcal{SH}$ [structurally stable case, $(n_0, n_1) = (1,1)$], the linking number of this axis with an unstable periodic orbit is its period p. As w moves outward, it makes a series of p intersections with this unstable periodic orbit. The order in which the intersections occur is determined by kneading theory [10]. At each intersection: (1) the linking number of the orbit with w decreases by one and (2) two symbols ^ in the cover change to ‾. We illustrate these ideas with a simple example. This is the perestroika of the lift of the period four orbit 0111 in the period doubling cascade in $\mathcal{SH}$. It lifts undergo the following perestroika:

$$(1,1) \quad \mathcal{D} \quad \hat{0}_l \hat{1}_r \hat{1}_l \hat{1}_r \quad \text{and} \quad \hat{0}_r \hat{1}_l \hat{1}_r \hat{1}_l$$

$$(0,1) \quad \mathcal{L} \quad \bar{0}_l \hat{1}_l \hat{1}_r \hat{1}_l \bar{0}_r \hat{1}_r \hat{1}_l \hat{1}_r$$

$$\mathcal{L} + 2\mathcal{SH} \quad \bar{0}_l \hat{1}_l \bar{1}_r \hat{1}_r \quad \text{and} \quad \bar{0}_r \hat{1}_r \bar{1}_l \hat{1}_l$$

$$\mathcal{L} + 2\mathcal{SH} \quad \bar{0}_l \bar{1}_l \bar{1}_l \hat{1}_l \bar{0}_r \bar{1}_r \bar{1}_r \hat{1}_r$$

$$(0,0) \quad 2\mathcal{SH} \quad \bar{0}_l \bar{1}_l \bar{1}_l \bar{1}_l \quad \text{and} \quad \bar{0}_r \bar{1}_r \bar{1}_r \bar{1}_r.$$

We point out the strong coupling between the left-right symbols l and r and the topological symbols ^ and ‾. That is, ^ forces the change $l \rightarrow r$, $r \rightarrow l$ while ‾ forces $l \rightarrow l$, $r \rightarrow r$.
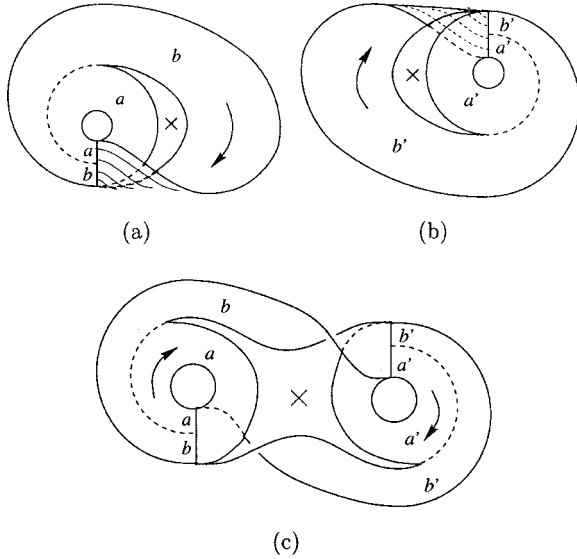
FIG. 12. (a) Image Smale horseshoe template. (b) Inversion image. (c) Double cover with inversion symmetry. The image of the rotation axis $(n_0,n_1)=(0,1)$ passes through ×.

VIII. ALGEBRAIC DESCRIPTION OF BRANCHED MANIFOLDS

Every branched manifold can be described by a set of integers. A template with n branches is described by the following arrays [4]:

(i) T: This is an $n \times n$ Markov transition matrix with entries 0 or 1. It describes the connectivity of the branched manifold. T_{ij} is 1 if branch i flows into branch j, 0 otherwise.

(ii) L: This is also an $n \times n$ matrix. It describes the topological organization of the branches. L_{ij} describes how branches i and j are intertwined. It is the algebraic sum of the signed crossings of the two branches $(i \ne j)$. L_{ii} is the torsion of branch i. It is the algebraic sum of the signed crossings of the two edges of branch i.

(iii) A: This is a $1 \times n$ array. It describes the order in which branches are joined at a branch line. When branches i and j meet at a branch line, $A_i < A_j$ if branch i is closer to the observer than branch j in the projection adopted.

For the Smale horseshoe shown in Fig. 12(a) we have

$$T=\begin{bmatrix} 1 & 1 \\ 1 & 1 \end{bmatrix} \quad L=\begin{bmatrix} 0 & 0 \\ 0 & +1 \end{bmatrix} \quad A=[+1 \ -1]. \quad (21)$$

Here the first row/column refers to branch a with local torsion 0 and the second to branch b with local torsion $+1$.

The Smale horseshoe template has many inequivalent twofold covers, depending on the symmetry group $\mathcal{G}$ $[=\mathcal{R}_z(\pi)$ or $\mathcal{P}]$ and the topological indices (n_0,n_1). The algebraic description of the covering branched manifold can be constructed from the algebraic description of the image branched manifold once the group $\mathcal{G}$ and indices (n_0,n_1) have been specified. We illustrate the algorithm involved by constructing the algebraic description of a twofold cover of

the Smale horseshoe template. The cover has inversion symmetry and the topological index for the horseshoe is $(n_0,n_1)=(0,1)$.

The image horseshoe is shown in Fig. 12(a). Its algebraic description is presented in Eq. (21). The branches are labeled a (first row/column, no torsion) and b (second row/column, torsion $=+1$). A second horseshoe is now created by applying the inversion operation to the first. This is shown in Fig. 12(b). Its algebraic description is

$$T=\begin{bmatrix} 1 & 1 \\ 1 & 1 \end{bmatrix} \quad L=\begin{bmatrix} 0 & 0 \\ 0 & -1 \end{bmatrix} \quad A=[-1 \ +1]. \quad (22)$$

The first and second rows/columns label branches a',b' with torsion 0, -1.

These two branched manifolds are now joined by rearranging their branches. The topological index (n_0,n_1) $=(0,1)$ provides the information required. Since $n_a=0$, branch a continues to flow into branches a,b. Similarly, $n_{a'}=0$ means branch a' continues to flow into branches a',b'. Since $n_1=1$, the period one orbit in branch b lifts to a trajectory in a cover, which cannot be closed (half a closed orbit). In other words, branch b now flows into branches a',b'. Similarly, branch b' flows into a,b. The Markov transition matrix is

$$T=\begin{bmatrix} 1 & 1 & 0 & 0 \\ 0 & 0 & 1 & 1 \\ 0 & 0 & 1 & 1 \\ 1 & 1 & 0 & 0 \end{bmatrix} \begin{matrix} a \\ b \\ a' \\ b' \end{matrix} \quad L=\begin{bmatrix} 0 & 0 & 0 & 0 \\ 0 & +1 & 0 & 0 \\ 0 & 0 & 0 & 0 \\ 0 & 0 & 0 & -1 \end{bmatrix}. \quad (23)$$

The linking matrix is the direct sum of the linking matrices for the pair of two-branch Smale horseshoe templates. It is also presented in Eq. (23).

The 1×4 array matrix is constructed as follows. For the two Smale horseshoe templates, $A_a > A_b$ and $A_{a'} < A_{b'}$. Branch b now joins branch a', so $A_{a'} > A_b$. Similarly $A_a < A_{b'}$. The following array satisfies these conditions:

$$A=[1 -2 -1 +2]. \quad (24)$$

The values of the array elements are not unique. Only their ordering is important.

The topological entropy of a branched manifold is obtained in the usual way from its transition matrix. It is the logarithm of the largest eigenvalue of T. For the Smale horseshoe template the eigenvalues of T are 2 and 0. For its double cover shown above, the eigenvalues are 2, 0, 0, and 0. Therefore, both the image and its cover shown here have the same topological entropy: $h_T = \ln 2$. It is possible to show that the topological entropy is unchanged under the cover-image relation. However, one must be careful. We illustrate a subtlety that can occur. The three $\mathcal{P}$-equivariant double covers of Fig. 8 have two branch lines each. The Poincaré section for each attractor is the union of the two branch lines. The attractors Figs. 8(a) and 8(b) each have period one orbits, while Fig. 8(c) has none. In fact, Fig. 8(c) has orbits of only "even period." However, for Fig. 8(c) it is possible to

slide one branch line around until it reaches the other. One then finds a branched manifold with four branches and one branch line. In this four-branch template, one period corresponds to propagation from the one branch back to itself. The topological entropy is $h_T = \ln 4$. If one redefines period in the original branched manifold [Fig. 8(c)] so that one period corresponds to propagation from one branch line through the second and back to the first, then the topological entropy is also redefined by a factor of $2: h_T = 2 \ln 2$.

IX. SUMMARY AND CONCLUSIONS

There is a general theory of image and cover dynamical system in $\mathbb{R}^n$. These are locally diffeomorphic dynamical systems, which are not globally diffeomorphic. The cover dynamical system is equivariant (unchanged) under a discrete symmetry group $\mathcal{G}$. The image dynamical system either has no residual symmetry, or is equivariant under a smaller group, a subgroup of $\mathcal{G}$. A change of coordinates performs the function of modding out the symmetry. This change of coordinates projects the cover to the image dynamical system. It is possible to ''lift'' an image dynamical system to a covering dynamical system by constructing the inverse transformation. An image dynamical system can have many inequivalent covering dynamical systems. They are distinguished among themselves by certain topological indices.

We have studied the cover-image, or project and lift, relation for three-dimensional dynamical systems that are equivariant under the two two-element groups $\mathcal{R}_z(\pi), \mathcal{P}$. In particular, the Lorenz and Burke and Shaw dynamical systems are equivariant under $\mathcal{R}_z(\pi)$. We constructed the image dynamical systems for each in Sec. III. The induced, Lorenz system and the Kremliovsky system are equivariant under $\mathcal{P}$. We have projected both to their image systems in Sec. IV.

We have presented: the equations, the strange attractors generated by the equations for certain parameter values, and a template or branched manifold which identifies the strange attractor.

We studied the problem of constructing covers from image dynamical systems by constructing branched manifolds that covered the Smale horseshoe template. The latter is a branched manifold with two branches. Its twofold covers have four branches. Four inequivalent covers with rotation symmetry were presented in Sec. V. These are distinguished by the topological index (n_0, n_1) where n_i is the linking number between the image of the rotation axis and branch i of the horseshoe template. One of these is disconnected.

A new global bifurcation has been described. It occurs when an image dynamical system is lifted to a covering dynamical system and the singular set of the local diffeomorphism is not bounded away from the flow in the image. This bifurcation has been illustrated on lifts of the displaced Rössler system with twofold rotation symmetry. In Sec. VI we studied three connected covers with inversion symmetry.

Branched manifolds are described by integers. The algebraic descriptions of cover and image branched manifolds are closely related. We showed how to construct the algebraic description of a cover from an image given: the algebraic description of the image, the group $\mathcal{G}$, and the topological index $(n_0, n_1, \ldots)$. This was done in Sec. VIII for the cover of the Smale horseshoe with topological index $(n_0, n_1) = (0,1)$ and inversion symmetry.

[1] E. N. Lorenz, J. Atmos. Sci. **20**, 130 (1963).
[2] O. E. Rössler, Phys. Lett. A **57**, 397 (1976).
[3] C. Letellier and G. Gouesbet, J. Phys. II **6**, 1615 (1996).
[4] R. Gilmore, Rev. Mod. Phys. **70** (4), 1455 (1998).
[5] D. A. Cox, J. B. Little, and D. O'Shea, *Ideals, Varieties and Algorithms* (Springer-Verlag, New York, 1996).
[6] R. Miranda and E. Stone, Phys. Lett. A **178**, 105 (1993).
[7] R. Shaw, Z. Naturforsch. A **36A**, 80 (1981).
[8] M. Kremliovsky (private communication).
[9] R. Gilmore and J. W. L. McCallum, Phys. Rev. E **51**, 935 (1995).
[10] P. Collet and J. P. Eckmann, in *Iterated Maps on the Interval as Dynamical Systems*, Progress in Physics, Edited by A. Jaffe et D. Ruelle (Birkhäuser, Boston, 1980).